Electron spin polarization in an excited triplet–radical pair system: Generation and decay of the state

ARTICLE *in* APPLIED MAGNETIC RESONANCE · JUNE 2006

Impact Factor: 1.17 · DOI: 10.1007/BF03166222

Appl. Magn. Reson. 30, 619–636 (2006)

Applied Magnetic Resonance

Electron Spin Polarization in an Excited Triplet-Radical Pair System: Generation and Decay of the State

V. F. Tarasov[1], I. S. M. Saiful[2], Y. Iwasaki[2], Y. Ohba[2], A. Savitsky[3], K. Möbius[3], and S. Yamauchi[2]

[1] Institute of Chemical Physics, Russian Academy of Sciences, Moscow, Russian Federation
[2] Institute of Multidisciplinary Research for Advanced Materials, Tohoku University, Sendai, Japan
[3] Institute of Experimental Physics, Free University Berlin, Berlin, Germany

Received July 11, 2006

Abstract. A computational model to simulate electron spin polarization in the three-spin-1/2 system composed of the molecular excited triplet state of (tetraphenylporphinato)zinc(II) (ZnTPP) and the doublet ground state of the 3-(N-nitronyl-notroxide) pyridine (3-NOPy) stable radical is proposed. The model is based on numerical solutions of the stochastic Liouville equation for the diffusively rotating system where the magnetic dipolar, isotropic Heisenberg exchange, and anisotropic Zeeman electron spin interactions are taken into account in a full measure, whereas the intersystem crossing processes between the singlet and triplet states of ZnTPP are considered in terms of kinetic equations for the relevant spin density matrices. Additional longitudinal and transversal paramagnetic relaxation caused by relative rotation motions of the ZnTPP and 3-NOPy moieties is taken into consideration in the form of the generalized relaxation operator.

1 Introduction

At the outset, interests in the three-spin-1/2 systems were rooted in the mechanism of perturbation of the singlet–triplet spin-forbidden transitions between electronically excited molecular states (enhanced intersystem crossing) by neighboring paramagnetic molecules. Hoijtink [1], Murrell [2], Robinson [3], and Chiu [4] have interpreted this mechanism in terms of exchange interactions in encounter complexes of molecular triplets and radicals. The "third-spin" effects on the spin evolution in radical pairs [5–7] and chemically induced dynamic electron polarization (CIDEP) in radicals escaped from encounters with molecular triplets [8–12] have rekindled this interest. The radical-triplet pair mechanism (RTPM) [8, 13] and the electron spin polarization transfer (ESPT) [14, 15] have been suggested to account for the latter. The essence of RTPM [13] is that the modulated Heisenberg electron spin–spin exchange interaction between a molecular triplet and a radical by translational diffusion and the modulated zero-field split-

ting (ZFS) in the triplet by rotational diffusion cause inherent population and/or depopulation of the spin states of an encounter complex. The efficiency of this process depends on which spin states are occupied by the encountering species. To our knowledge, no specific details for ESPT have been suggested. For both phenomena, CIDEP of purely free radicals escaped from encounters is observed in a time-resolved electron paramagnetic resonance (TREPR) experiment. The durations of the diffusive encounters in ordinary liquid solutions are too short and disturbances of the spin states of molecular triplets are too small to observe both the encounter complexes themselves or changes in the populations of molecular triplet spin states. In addition, detection of TREPR spectra from individual molecular excited triplets in liquid solution was believed to be impossible for years because of fast paramagnetic relaxation in the rotating molecular triplet.

Nevertheless, not so long ago TREPR spectra of such molecular triplets of fullerene C_{60} [16, 17] and tetraphenylporphyrins [15] were successfully detected in liquid solvents. Moreover, Corvaja et al. [18] and Yamauchi et al. [19] have observed excited quartet states of C_{60} and both excited doublet and quartet spin states of metal porphyrins ligated by stable nitroxide radicals in fluid solution, respectively. In either case the molecular excited states were spin-polarized, i.e., the intensity of the TREPR signals exceeded those provided by Boltzmann (thermal) polarization of electron spins and were in either an absorptive or an emissive mode. To differentiate this phenomenon from the CIDEP due to the triplet mechanism (TM), RTPM, and ESPT, we use the term triplet-radical electron spin polarization or TR-ESP. These experimental observations have opened, among other things, a new avenue of attack on the problem of an enhanced intersystem crossing and CIDEP due to triplet–radical encounters.

Qualitative interpretation [19] of the TR-ESP was based on an idea that the forbidden intersystem crossing between singlet and triplet states in a molecule is converted into allowed transitions between states of the same multiplicity when a stable radical is bound to a molecule. In fact, while this could explain the sign of TR-ESP at comparatively earlier times (RTPM-like polarization), it is not able to interpret the changes of ESP signs at longer times. A more rigorous theoretical description of the TREPR spectra of molecular triplets ligated with stable nitroxide radicals has been realized only for the case of solid solutions [20, 21]. However, this approach is of little use as applied to kinetics of TR-ESP observed in liquid solutions. To describe the kinetic characteristics of the spectra, it was suggested to apply either the modified Bloch equations [22] or the kinetic equations for populations and depopulations [23]. These approaches have been successfully utilized to interpret effects of the fast intersystem processes and estimate their rate constants. At the same time they suffer from too many kinetic parameters involved, while the necessity of some of these parameters could be substantiated only rather arbitrarily.

In this paper, we suggest a computational model describing the evolution of TR-ESP in systems like (tetraphenylporphinato)zinc(II) (ZnTPP) ligated by the stable nitroxide radical 3-(N-nitronyl-notroxide) pyridine (3-NOPy). The magnetic dipolar, isotropic Heisenberg exchange, and anisotropic Zeeman electron spin

interactions are taken into account in a full measure. In this aspect, we follow the theory for the transient EPR spectra of coupled three-spin systems developed by Salikhov, van der Est, and Stehlik [24]. The model is based on the stochastic Liouville equation (SLE) as applied to the diffusively rotating system where the intersystem crossing processes, "spin-selective" and "spin-nonselective", between the singlet and triplet states of ZnTPP are considered in terms of a kinetic approach. To take into account an additional longitudinal and transversal paramagnetic relaxation caused by relative motions of the ZnTPP and 3-NOPy moieties, we use the generalized relaxation matrix constructed in such a way that the spin systems of ZnTPP and 3-NOPy approach to their equilibrium. This theoretical approach, as is shown in the paper, allows excellent fits to the experimental results and to estimate the order of spin selectivity of the intersystem crossing in the system considered.

2 Brief Discussion of Experimental Results

The chemical structure of ZnTPP ligated with 3-NOPy is shown in Fig. 1. The energy level diagram of this complex has been discussed previously [25]. Figure 2 shows the diagram and the nomenclature used in the present paper. The W-band TREPR spectrum of the ZnTPP-3-NOPy complex observed at room temperature in toluene and at 100 ns delay time after the laser pulse is shown in Fig. 3. The spectrum has been exhaustively characterized earlier [25]. It is composed of three signals. The three-line signal (D_0) centered at $g = 2.0059$ is assigned to EPR transitions in the ground state of the ZnTPP-3-NOPy complex. The separate signal positioned at $g = 2.0031$ and labeled by Q_1 is due to EPR transitions within the molecular excited quartet state. The much weaker signal labeled as D_1 is characterized by $g = 2.0005$ and has been proved [19] to be due to the excited doublet state of the complex.

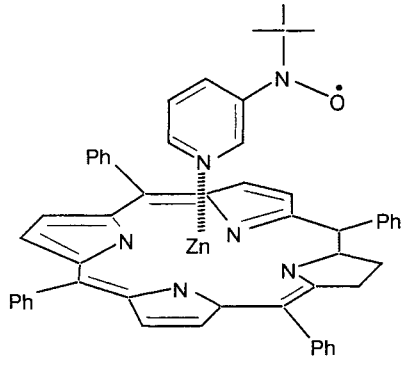

Fig. 1. Molecular structure of the ZnTPP-3-NOPy complex. The *Z*-axis of the molecular frame is directed perpendicularly to the ZnTPP plane.

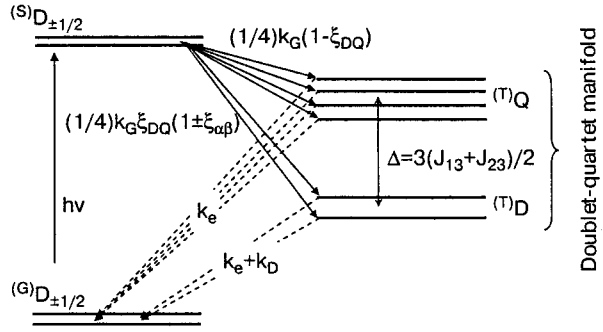

Fig. 2. Energy level diagram and the nomenclature of the transitions that are described kinetically in the ZnTPP-3NOPy complex.

Time profiles of these three signals normalized to unit intensities observed at their positive maxima are shown in Fig. 4. We recognize three major peculiarities of the time profiles. First, while the intensity of the Q_1 signal at maximum far exceeds that of D_1 [26], within the experimental noise the normalized time profiles of the Q_1 and D_1 signals are similar to each other. The D_1 signal shows slightly faster growth at initial times. To some extent the differences can be attributed to a wider spectral shape of the D_1 signal [25, 26] and to higher spectral transition probability of the Q_1 signal [19]. Second, both the Q_1 and D_1 signals are positively polarized initially, they peak at about 20–25 ns, then change their signs at about 75–85 ns, reach their negative peak at 130–140 ns, and finally tend to zero roughly exponentially with the time constant of ca. 100 ns. Third, the time profile of the D_0 signal (3-NOPy) is more complex. For the sake of convenience we split the time interval of observations into three parts. Part I includes the negative initial ESP which peaks at 20 ns. Part II includes the growth

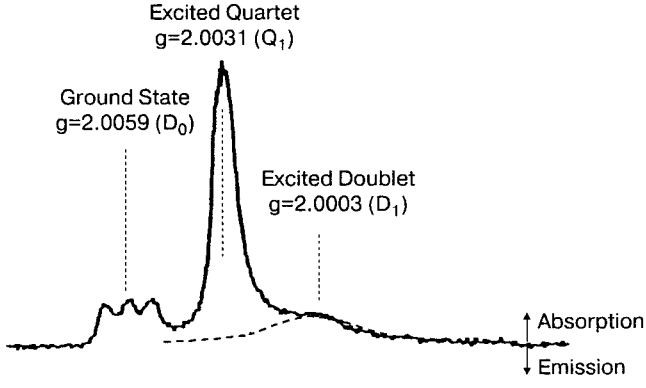

Fig. 3. W-band (95 GHz) EPR spectrum of the ZnTPP-3-NOPy complex observed in toluene at room temperature and 100–150 ns after the laser pulse.

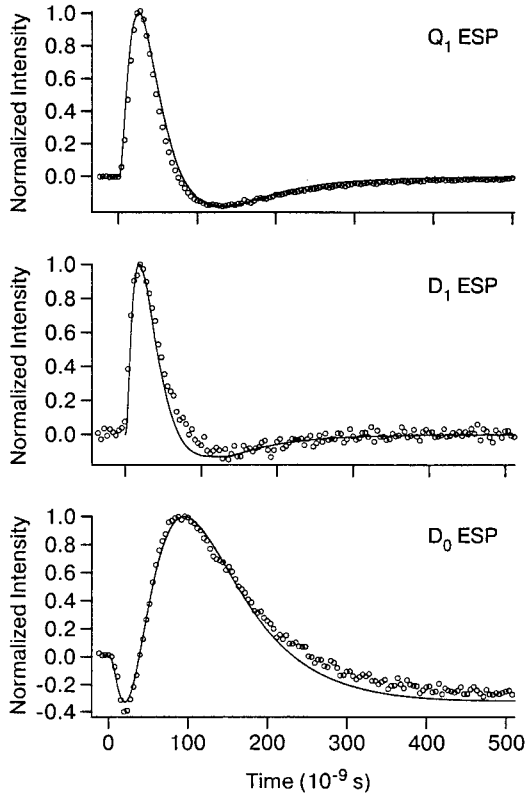

Fig. 4. W-band EPR time profiles of the Q_1, D_1, and D_0 signals of the ZnTPP-3-NOPy complex in toluene at room temperature and the resonance fields marked by vertical dashed lines in Fig. 3 (open circles). The numerical simulations are shown by the solid lines with the parameters: $J_e = -34$ GHz, $k_D = 2.1 \cdot 10^7$ s^{-1}, $k_e = 7.5 \cdot 10^6$ s^{-1}, $k_{rel} = 1.92 \cdot 10^7$ s^{-1}, $\xi_{DQ} = 0.68$, $\xi_{\alpha\beta} = -0.02$; other parameters are listed in the text.

of positive ESP peaked at 90 ns, and its decay including the time of second change of the ESP sign at about 250 ns. It is interesting that the decay of the ESP can be approximated by the same monoexponential rate of 10^7 s^{-1}. In part III, the negatively polarized EPR signal peaks at 500 ns and finally decays slowly to zero (minus Boltzmann equilibrium polarization) with the approximate exponential rate of ca. $8 \cdot 10^5$ s^{-1}, which is most likely to be the longitudinal relaxation rate of the 3-NOPy radical part. Solid lines in Fig. 4 are computational fits.

3 Computational Model

In this paper, we intend to interpret quantitatively the time profiles of EPR signals presented in Fig. 4. To do this, we apply the SLE to the ZnTPP-3-NOPy

complex considered as an isotropic solid diffusing rotationally in isotropic media. Solidity means here constant relative orientation of the ZnTPP and 3-NOPy moieties. Taking the rotational diffusion into account, the effects of anisotropic magnetic interactions, such as the Zeeman interactions and ZFS, are considered tentatively. In our case, this is of great importance, since we deal with a multilevel system where the energy splitting and crossing depend strongly on the electron spin–spin Heisenberg exchange interactions.

We start with the assumption that the system under consideration is composed of the three spins 1/2. While two spins S_1 and S_2 are supposed to be located in ZnTPP, the third spin S_3 is located in the 3-NOPy moiety. For the sake of simplicity, we assume that the necessary spin-orbital wave functions can be written as antisymmetrized linear combinations of the products $|\phi_a(1),\phi_b(2),\phi_R(3)\rangle \times |\chi_m(1),\chi_m(2),\chi_m(3)\rangle$, where ϕ_a and ϕ_b are the molecular orbital (MO) wave functions of the two spins of the ZnTPP moiety. Although the structure of the ZnTPP electronic configurations is more complex [20], only one of the two excited doublet states of the ZnTPP-3-NOPy complex is involved in the intersystem crossing process [20]. ϕ_R is the ground state singly occupied MO of the 3-NOPy, χ_m is the ordinary spin 1/2 wavefunction ($m = \pm 1/2$). These suggestions allow for expressing the contributions from the exchange interaction in the ZnTPP-3-NOPy complex in terms of the Hamiltonian

$$\hat{\mathscr{H}}_{ex} = -\sum_{i<j} J_{ij}(1/2 + 2\hat{\mathbf{S}}_i\hat{\mathbf{S}}_j) = -J_{12}\cdot(1/2 + 2\hat{\mathbf{S}}_1\hat{\mathbf{S}}_2) - (J_{13} + J_{23})(1/2 + [\hat{\mathbf{S}}_1 + \hat{\mathbf{S}}_2]\hat{\mathbf{S}}_3) - (J_{13} - J_{23})(\hat{\mathbf{S}}_1 - \hat{\mathbf{S}}_2)\hat{\mathbf{S}}_3, \quad (1)$$

where J_{ij} are the corresponding exchange integrals. In an effort to interpret experimental observations, it is convenient to use the set (Q-basis) $|^{(T)}Q_{\pm 3/2}\rangle$, $|^{(T)}Q_{\pm 1/2}\rangle$, $|^{(T)}D_{\pm 1/2}\rangle$, $|^{(S)}D_{\pm 1/2}\rangle$ of the spin functions which are the eigenfunctions of the total spin $\mathbf{F} = \hat{\mathbf{s}}_1 + \hat{\mathbf{s}}_2 + \hat{\mathbf{s}}_3$. It seems reasonable to suggest that $|J_{12}| \gg \max\{|J_{13}|,|J_{23}|\}$, which indicates in its turn the rational scheme of the spin addition as $(\hat{\mathbf{s}}_1 + \hat{\mathbf{s}}_2) + \hat{\mathbf{s}}_3$, i.e.,

$$|^{(T)}Q_{\pm 3/2}\rangle = |T_{\pm 1}\rangle|\pm 1/2\rangle, \quad (2a)$$

$$|^{(T)}Q_{\pm 1/2}\rangle = \sqrt{2/3}\,|T_0\rangle|\pm 1/2\rangle + \sqrt{1/3}\,|T_{\pm}\rangle|\mp 1/2\rangle, \quad (2b)$$

$$|^{(T)}D_{\pm 1/2}\rangle = \pm\sqrt{2/3}\,|T_{\pm}\rangle|\mp 1/2\rangle \mp \sqrt{1/3}\,|T_0\rangle|\pm 1/2\rangle, \quad (2c)$$

$$|^{(S)}D_{\pm 1/2}\rangle = |S\rangle|\pm 1/2\rangle, \quad (2d)$$

where $|T_{\pm}\rangle$, $|T_0\rangle$, and $|S\rangle$ are the ordinary triplet and singlet spin wave functions of the porphyrin part. While the spin functions $|^{(T)}Q_{\pm 3/2}\rangle$ and $|^{(T)}Q_{\pm 1/2}\rangle$ are the eigenfunctions of the exchange Hamiltonian Eq. (1), the spin functions $|^{(T)}D_{\pm 1/2}\rangle$ and $|^{(S)}D_{\pm 1/2}\rangle$ are mixed by exchange interactions because of the following nonzero off-diagonal elements $\langle^{(S)}D_{\pm 1/2}|\hat{\mathscr{H}}_{ex}|^{(T)}D_{\pm 1/2}\rangle = (\sqrt{3}/2)(J_{13} - J_{23})$. This mixing forms the basis for allowing the forbidden singlet–triplet transitions of the ZnTPP

moiety to "borrow" [4] or to "steal" [1] the intensity from the allowed singlet–singlet transition. With the expected, but not yet tested, constraint $|J_{12}| \gg \max\{|J_{13}|,|J_{23}|\}$, this mixing can be neglected in first approximation, i.e., the excited doublet states $|^{(S)}D_{\pm 1/2}\rangle = |S\rangle|\pm 1/2\rangle$ of the ZnTPP-3-NOPy complex are well separated from the doublet-quartet manifolds of the spin states generated by coupling of the excited triplet of ZnTPP and the 3-NOPy radical.

By this approximation we leave out the ground $^{(G)}D_{\pm 1/2}$ and excited $|^{(S)}D_{\pm 1/2}\rangle$ doublet spin states from consideration of spin evolution. The remaining six-dimension spin space of the spin states $|^{(T)}Q_{\pm 3/2}\rangle$, $|^{(T)}Q_{\pm 1/2}\rangle$ and $|^{(T)}D_{\pm 1/2}\rangle$ is called the doublet-quartet manifolds.

The magnetic dipole–dipole interaction in a three-spin system is given by

$$\mathscr{H}_{\text{dip}} = \mu_B^2 g^2 \sum_{i<j} \left(\frac{\hat{\mathbf{s}}_i \cdot \hat{\mathbf{s}}_j}{r_{ij}^3} - 3\frac{(\hat{\mathbf{s}}_i \cdot \hat{\mathbf{r}}_{ij})(\hat{\mathbf{s}}_j \cdot \hat{\mathbf{r}}_{ij})}{r_{ij}^5} \right), \qquad i, j = 1, 2, 3, \tag{3}$$

where μ_B is the electron Bohr magneton, g (=2.0023) is the free electron g-factor, $\hat{\mathbf{r}}_{ij}$ represent mutual spatial coordinates of electrons. Taking into account the above discussion, neglecting the overlap of the orbital wave functions and suggesting that $\langle r_{13}\rangle = \langle r_{23}\rangle \approx r_{\text{TR}} \gg \langle r_{12}\rangle$, one obtains [29] the dipolar Hamiltonian

$$\hat{\mathscr{H}}_{\text{dip}} = \hat{\mathbf{T}} \cdot D_{\text{ZFS}} \cdot \hat{\mathbf{T}} + \hat{\mathbf{T}} \cdot D_{\text{pd}} \cdot \hat{\mathbf{s}}_3 , \tag{4}$$

where D_{ZFS} and D_{pd} are the corresponding fine structure tensors. In their eigenframes, they are

$$D_{\text{ZFS}} = \begin{pmatrix} E_T - D_T/3 & 0 & 0 \\ 0 & -E_T - D_T/3 & 0 \\ 0 & 0 & 2D_T/3 \end{pmatrix},$$

$$D_{\text{pd}} = \frac{\mu_B^2}{r_{\text{TR}}^3} g^2 \cdot \begin{pmatrix} 1 & 0 & 0 \\ 0 & 1 & 0 \\ 0 & 0 & -2 \end{pmatrix}, \tag{5}$$

where E_T and D_T are the ZFS parameters for the ZnTPP triplet. Note that the assumption $r_{\text{TR}} \gg \langle r_{12}\rangle$ is equivalent to the inequality $(g^2\mu_B^2)/r_{\text{RT}}^3 \ll |D_T|$, i.e., the total magnetic dipolar interaction in the given system can be represented by Eq. (4) if the magnetic interaction between the triplet state electrons of the ZnTPP moiety and the doublet state electron of the 3-NOPy moiety is much smaller than that within the triplet state.

Another way of looking at the magnetic dipolar interactions in the ZnTPP-3-NOPy complex is to introduce the fine structure tensor for pure quartet states, i.e., to replace the Hamiltonian Eq. (4) with the Hamiltonian

$$^{(Q)}\hat{\mathscr{H}}_{dip} = D_Q(\hat{F}_z^2 - \hat{\mathbf{F}}^2/3) + E_Q(\hat{F}_x^2 - \hat{F}_y^2)\,.$$

Estimates for the ZFS parameters D_Q and E_Q for the quartet manifold are given in ref. 20. In the present work, we use the Hamiltonian described by Eqs. (4) and (5). This will allow us to recognize the importance of the magnetic dipolar interaction between the electron spins of the porphyrin and radical moieties.

The Zeeman interactions with the external magnetic field $\mathbf{B}_0$ of the spectrometer are described by the Hamiltonian

$$\hat{\mathscr{H}}_Z = \mu_B \mathbf{B}_0 \cdot (\mathbf{g}_R \cdot \hat{\mathbf{S}}_R + \mathbf{g}_T \cdot \hat{\mathbf{T}})\,, \tag{6}$$

where $\mathbf{g}_R$ and $\mathbf{g}_T$ are the g-tensors of 3-NOPy and the ZnTPP triplet, respectively.

According to the approximations, in the Liouvillian spin space the spin state vector of the ZnTPP-3-NOPy complex is composed of the two four-dimensional state vectors describing the doublet ground $^{(G)}\boldsymbol{\rho}_D(t)$ and excited $^{(S)}\boldsymbol{\rho}_D(t)$ electronic states and the thirty six-dimensional state vectors of the doublet-quartet manifolds. All these state vectors depend on the orientation of the ZnTPP-3-NOPy complex (molecular frame), g-tensors, and D_{pd} with respect to the magnetic field $\mathbf{B}_0$ and the mutual orientations of the relevant tensors.

Time evolution of the state vector $^{(T)}\boldsymbol{\rho}_{DQ}(t)$ describing the doublet-quartet manifolds in the complex obeys the SLE

$$\frac{d\,^{(T)}\boldsymbol{\rho}_{DQ}}{dt} = (-i\hat{\hat{\mathscr{H}}} + \hat{\hat{R}} - \hat{\hat{K}} + D_{rot}\nabla^2) \cdot {}^{(T)}\boldsymbol{\rho}_{DQ} + \hat{\hat{G}}\,{}^{(S)}\boldsymbol{\rho}_D\,. \tag{7}$$

In the Liouvillian spin space, the spin Hamiltonian of the ZnTPP-3-NOPy complex is described by the superoperator $\hat{\hat{\mathscr{H}}}$, which is the sum of superoperators $\hat{\hat{\mathscr{H}}} = \hat{\hat{\mathscr{H}}}_{ex} + \hat{\hat{\mathscr{H}}}_{dip} + \hat{\hat{\mathscr{H}}}_Z$ generated by Eqs. (1), (4) and (6).

$D_{rot}\nabla^2$ is the diffusion operator with D_{rot} being the rotational diffusion coefficient, $D_{rot} = (1/6)\tau_c$. τ_c is the rotational correlation time of the ZnTPP-3-NOPy complex. In fact, the 3-NOPy moiety is not entirely fixed with respect to the ZnTPP moiety, which means that there should be an additional correlation time for the restricted rotational motion of 3-NOPy itself. Nevertheless, for the sake of simplicity we consider the 3-NOPy moiety as if it was fixed with respect to ZnTPP. If the assumption $(g^2\mu_B^2)/r_{RT}^3 \ll |D_T|$ is fulfilled, this simplification cannot result in dramatic computational errors.

A relative motion of the two moieties modulates the magnitudes of exchange (J_{13}, J_{23}) and dipolar (D_{pd}) interactions. As a consequence, this motion causes additional paramagnetic relaxation (we call it internal relaxation). Since our computational resources are limited and parameters characterizing these interactions and mutual motions are poorly understood, the best representation of this additional relaxation can be expressed in terms of relaxation rates taken as fitting parameters, i.e., we construct the relaxation superoperator $\hat{\hat{R}}$ in the τ-basis ($|\tau_\mu(1,2)\chi_m(3)\rangle$; $\hat{S}_\mu\,|\tau_\mu(1,2)\rangle = 0$) in such a way that the triplet state of ZnTPP and

the doublet state of 3-NOPy relax to their equilibrium with the longitudinal and transversal rates k_{1T} and k_{2T}, and k_{1R} and k_{2R}, respectively (see appendix).

According to an earlier treatment [1–3], the singlet–triplet transition in ZnTPP must be replaced by the transition between the excited doublet subspace of the doublet-quartet manifolds and the doublet ground state. This treatment is justified if the dipolar interactions (including ZFS) are weak and the exchange interactions separating the excited doublet and quartet subspaces are strong enough. If such conditions are not fulfilled, we should include the transitions from the excited quartet states as well [4]. This is the reason why we construct the superoperator $\hat{K}$ describing the decay of the doublet-quartet manifolds as follows:

$$\hat{K}\,{}^{(T)}\boldsymbol{\rho}_{DQ} = k_e\,{}^{(T)}\boldsymbol{\rho}_{DQ} + \frac{k_D}{2}\{\hat{P}_D\,{}^{(T)}\boldsymbol{\rho}_{DQ} + {}^{(T)}\boldsymbol{\rho}_{DQ}\hat{P}_D\}, \tag{8}$$

where the superoperator $\hat{P}_D$ is the projector onto the doublet subspace of the doublet-quartet manifolds. As it follows from Eq. (8), we differentiate two types of the decay (Fig. 2): the k_D process is a "spin selective" decay, it involves only the doublet subspace of the doublet-quartet manifolds, the k_e process takes place irrespectively to all the states belonging to the doublet-quartet manifolds. For the case of weak disturbance of the singlet–triplet transition probability in ZnTPP by 3-NOPy, k_e can be interpreted as an intersystem crossing due to the spin–orbit coupling and k_D is due to the exchange type interaction.

The term $\hat{G}^{(S)}\boldsymbol{\rho}_D$ in Eq. (7) describes a population of the doublet-quartet manifolds via the depopulation of the excited doublet states $|^{(S)}D_{\pm 1/2}\rangle$ with the rates (Fig. 2) which are not necessary equal each other [19]. Since the intersystem crossing rate is rather fast, we restrict ourselves by formulation of specific initial conditions for the doublet-quartet manifolds:

$$\begin{aligned} &{}^{(T)}\rho_{DQ}(t=0) \\ &= \frac{1}{4}\begin{pmatrix} 1-\xi_{DQ} & & & & & & \\ & 1-\xi_{DQ} & & & & & \\ & & 1-\xi_{DQ} & & & & \\ & & & 1-\xi_{DQ} & & & \\ & & & & 2\xi_{DQ}(1+\xi_{\alpha\beta}) & & \\ & & & & & 2\xi_{DQ}(1-\xi_{\alpha\beta}) & \end{pmatrix}. \end{aligned} \tag{9}$$

By the same reason as for the depopulation of the doublet-quartet manifolds, we introduce the parameter ξ_{DQ} to describe the nonequivalence in the initial populations of the doublet and quartet subspaces. It appears reasonable that the initial population of the doublet subspace is higher than that of the quartet. According to Eq. (9), this preference in population means that $\xi_{DQ} > 1/3$.

In a strict sense the initial population must depend not only on whether the state belongs to the doublet or quartet state but also on the quantum numbers

m_z as well. Purely computationally we found that the calculated kinetics strongly depend on nonequivalence [19] in populating of the $|^{(T)}D_{+1/2}\rangle$ and $|^{(T)}D_{-1/2}\rangle$ spin states. To describe this nonequivalence, we introduce the parameter $\xi_{\alpha\beta}$. In the following, it is shown that $\xi_{\alpha\beta} < 0$ and $|\xi_{\alpha\beta}| \ll 1$, i.e., nonequivalence is rather small and the initial population of the $|^{(T)}D_{-1/2}\rangle$ spin state is slightly higher that that of the spin state $|^{(T)}D_{+1/2}\rangle$. At the same time, calculations are much less sensitive to the nonequivalence between states of the quartet subspace. For this reason we use the approximation that initially all the quartet sublevels are populated equally (Eq. (9)).

The state vector $^{(G)}\boldsymbol{\rho}_D(t)$ describes the ZnTPP-3-NOPy complex in its ground doublet state. We neglect the Boltzmann ESP in the 3-NOPy moiety. Therefore, the SLE for the state vector $^{(G)}\boldsymbol{\rho}_D(t)$ reads

$$\frac{d^{(G)}\boldsymbol{\rho}_D}{dt} = \mathrm{Tr}_{S_1,S_2}\{\hat{\hat{K}}^{(T)}\boldsymbol{\rho}_{DQ}\} + \hat{\hat{R}}^{(D)}\boldsymbol{\rho}_D, \tag{10}$$

i.e., we consider it as the product of the intersystem crossing between the double ground state and doublet-quartet manifolds. Instead of taking into account the anisotropic Zeeman and hyperfine interactions in the 3-NOPy radical, we use the Bloch-like relaxation superoperator $\hat{\hat{R}}^{(D)}$ with the same longitudinal and transversal relaxation rates k_{1RR} and k_{2RR} for any EPR transitions.

4 Simulation Procedure

Modeling of TR-ESP in the system considered is based on the suggestion that the statistical ensemble of the ZnTPP-3-NOPy complexes can be split so that each resultant subensemble $\boldsymbol{\sigma}_j$ is composed of complexes diffusing along approximately the same diffusion trajectory marked j. These subensembles are believed to include a sufficient amount of members, i.e., superoperators $\hat{\hat{K}}$ and $\hat{\hat{R}}$ can be used as in Eqs. (7) and (10). If each subensemble was composed of the only one complex, the specific algorithms [26] to model the decay and relaxation must be constructed.

To model rotational diffusion, we replace the continuous rotational diffusion with the rotational random walks. Such an approach has already been applied [28] to model the CIDEP due to RTPM. First of all, we adopt some small time interval δt which is considered as an element of time during which the complex is considered to be at rest. We use such short δt that the computational results do not depend essentially on its further shortening.

To model the populating process of the doublet-quartet manifolds, i.e., the $\hat{\hat{G}}^{(S)}\boldsymbol{\rho}_D$ term in Eq. (7), the computer generates a random number uniformly distributed within the interval [0,1]. If this number is larger than $\exp(-k_G\delta t)$, where k_G is the overall rate constant of depopulation of the excited doublet spin states $|^{(S)}D_{\pm 1/2}\rangle$, the doublet-triplet manifolds are considered to be populated according to the initial condition Eq. (9). In the opposite case, the procedure has

to be repeated. Finally, the initial time $\tau_0 = 0$ on the molecular time axis corresponds to the laboratory time $\tau_0 = (N_0 - 1)\delta t$, where N_0 is the number of unsuccessful attempts to start the spin and space evolution. This procedure provides the exponential decay of the excited doublet state $|^{(S)}D_{\pm 1/2}\rangle$ with the rate constant k_G.

Initial orientation of the ZnTPP-3-NOPy complex at $\tau_0 = 0$ is considered to be random in the laboratory frame. Geometrically, we consider the ZnTPP-3-NOPy complex as a spherical top diffusing rotationally in a homogeneous medium. At each moment of the molecular time $\tau_i = (i - 1)\delta t$ ($i = 1, 2, \ldots$) the orientation $\Omega^{(M_i)}(\tau_i)$ of the complex is given by the set of Euler angles {0,0,0} in the molecular frame. The diffusion is considered as a rotation around the axis $\mathbf{n}^{(M_i)}(\theta_i, \varphi_i)$ randomly oriented in the ith molecular frame through the random angle g_i distributed according to the well-known solution of the diffusion equation. In another way we use the rejection method to generate desirable distribution of random numbers $\gamma_i \in [0, \pi]$.

During each particular time interval $\{\tau_i, \tau_i + \delta t\}$ the propagation of the jth state vector in the laboratory frame $\{^{(T)}\sigma_{DQ}(\tau_i, \Omega_i^{(L)})\}_j$ is given by

$$\{^{(T)}\sigma_{DQ}(\tau_i + \delta t, \Omega_i^{(L)})\}_j = \exp\{\delta t(-i\hat{\hat{\mathscr{H}}} + \hat{\hat{R}} - \hat{\hat{K}})\}\{^{(T)}\sigma_{DQ}(\tau_i, \Omega_i^{(L)})\}_j . \quad (11)$$

To calculate the time propagation of the state vector $\{^{(G)}\sigma_D(t_i, \Omega_i^{(L)})\}_j$, we integrate Eq. (11) and get

$$\{^{(T)}\sigma_{DQ}(\tau_{i+1})\}_j - \{^{(T)}\sigma_{DQ}(\tau_i)\}_j = (-i\hat{\hat{\mathscr{H}}} + \hat{\hat{R}} - \hat{\hat{K}}) \cdot {}^{(T)}\{\tilde{\sigma}_{DQ}\}_j , \quad (12)$$

where

$$\{^{(T)}\tilde{\sigma}_{DQ}\}_j = \int_{\tau_i}^{\tau_i + \delta t} dt\, {}^{(T)}\{\sigma_{DQ}\}_j .$$

Then,

$$\{^{(T)}\tilde{\sigma}_{DQ}\}_j = (-i\hat{\hat{\mathscr{H}}} + \hat{\hat{R}} - \hat{\hat{K}})^{-1}(\{^{(T)}\sigma_{DQ}(\tau_{i+1})\}_j - \{^{(T)}\sigma_{DQ}(\tau_i)\}_j) . \quad (13)$$

Insertion of this solution into Eq. (12) gives

$$\int_{\tau_i}^{\tau_{i+1}} \frac{d\{^{(G)}\sigma_D\}_j}{dt} dt = \{^{(G)}\sigma_D(\tau_{i+1})\}_j - \{^{(G)}\sigma_D(\tau_i)\}_j$$
$$= Tr_{S_1,S_2}\{\hat{\hat{K}}\, {}^{(T)}\{\tilde{\sigma}_{DQ}\}_j\} + \hat{\hat{R}}\, {}^{(D)}\{\tilde{\sigma}_D\}_j . \quad (14)$$

Equation (14) allows for calculations of the state vector $\{^{(G)}\sigma_D(\tau_{i+1})\}_j$ since the state vector $\{^{(G)}\sigma_D(\tau_i)\}_j$ has been calculated in the previous walk.

In order to obtain solutions to Eqs. (7) and (10), one has to average $\{^{(T)}\sigma_{DQ}(\tau_i,\Omega_i^{(L)})\}_j$ and $\{^{(G)}\sigma_D(\tau_i)\}_j$ over many $j = 1, \ldots, N_{tr}$ diffusion trajectories $N_{tr} \gg 1$. Averaging should be performed in the laboratory time, so that

$$^{(T)}\rho(t_i,\Omega_i^{(L)}) \cong \left\langle ^{(T)}\sigma_{DQ}(t_i,\Omega_i^{(L)})\right\rangle = \frac{1}{N_{tr}}\sum_{j}^{N_{tr}}\{^{(T)}\sigma_{DQ}(t_i - t_{0j},\Omega_i^{(L)})\}_j , \qquad (15)$$

where t_{0j} is the initial time of the random walks along the jth trajectory in the laboratory time axis. The average state vector $\langle^{(G)}\sigma_D(t_i,\Omega_i^{(L)})\rangle$ is obtained in a similar fashion. Computed state vectors allow for computation of the longitudinal magnetizations of the doublet and quartet states of the double-quartet manifolds and the longitudinal magnetization of the ground doublet state. The EPR signals Q_1, D_1, and D_0 are supposed to be proportional to the corresponding magnetizations of the states.

5 Discussion of the Simulation Results

Solid lines in Fig. 4 are the kinetic traces computed according to the procedure described above. As may be inferred from Fig. 4 the model is quite capable of successful fitting of experimental results.

Invariable parameters. Amongst the parameters used in the calculations certain parameters were considered as invariable. This is the rotational correlation time $\tau_c = 150$ ps, which is quite close to the estimate based on the well-known relation $\tau_c = 4\pi a^3\eta/3k_BT$; all the symbols here are of standard meaning. For this correlation time, $\delta t = 40$ ps is such a time interval that its further decrease does not influence much the computational result. The ZFS parameters are $D_T = 1$ GHz and $E_T = 0.25$ GHz for the ZnTPP moiety, that are parameters of triplet ZnTPP [26]. Furthermore, there are the g-tensors for 3-NOPy and the ZnTPP triplet. For the 3-NOPy radical part, it was found that $g_{xx}^{(R)} = 2.0095$, $g_{yy}^{(R)} = 2.0058$, $g_{zz}^{(R)} = 2.0022$ (I. S. M. Saiful et al., unpubl.) with the Z-axis, pointing in the direction of the N 2p orbital in the SOMO and the XY-plane assumed to be perpendicular to the plane of the ZnTPP moiety. For the sake of simplicity, we neglect the anisotropy of the hyperfine interaction in this radical. The g-tensor of the ZnTPP triplet is less anisotropic ($g_{xx}^{(T)} = 2.003$, $g_{yy}^{(T)} = 2.003$, $g_{zz}^{(T)} = 1.998$) (I. S. M. Saiful et al., unpubl.) [30]. The computational curves were obtained under the condition of rather fast deactivation $k_G = 1.3 \cdot 10^8$ s^{-1} of the excited $|^{(S)}D_{\pm 1/2}\rangle$ spin states. Although this rate is much slower than the expected rate from the experimentally obtained lifetime of <40 ps [31] of the ZnTPP-3-NOPy fluorescence, further increase in the value k_G does not lead to any essential changes in the computation results. Therefore, the difference between the expected and used parameter values cannot be considered as contradiction.

Variable parameters. With the assumption $|J_{12}| \gg \max\{|J_{12}|,|J_{23}|\}$ and kinetic linking of the excited $|^{(S)}D_{\pm 1/2}\rangle$ and ground $|^{(G)}D_{\pm 1/2}\rangle$ spin states in the doublet-quartet manifolds $\{|^{(T)}Q_{\pm 3/2}\rangle, |^{(T)}Q_{\pm 1/2}\rangle, |^{(T)}D_{\pm 1/2}\rangle\}$, the intensity of the exchange in-

teraction J_{12} is of no importance. All the calculations were performed under the assumption that $J_{13} = J_{23} = J_e$. Traces in Fig. 4 were computed using $J_e = -34$ GHz. A negative sign of the exchange integral J_e is necessary [19] to get at least a qualitative agreement between experiments and computations. When $|J_e|$ exceeds 80 GHz, the enhancement factor of TR-ESP becomes too small relative to Boltzmann polarization. At the opposite limit $|J_e| < 16$ GHz, the computed ESP kinetics do not agree with the experiment even qualitatively. At $J_e \sim 32$ GHz, the enhancement factor reaches its maximum (about 10^3 relative to Boltzmann polarization).

From the chemical structure of the ZnTPP-3-NOPy complex, it is conceivable that the rough distance r_{TR} between the paramagnetic center of the 3-NOPy and ZnTPP moieties is around 0.6 nm. We would like to note again that $\mathbf{r}_{TR}$ is in fact not a fixed vector in the molecular frame due to the relative motion of these two moieties. When the distance r_{TR} was varied within the interval 0.5–0.7 nm, the agreement with experimental kinetics could be maintained by proper variation of other parameters.

As it was discussed above, we used the kinetic approach to describe the internal relaxation caused by relative motion of the ZnTPP and 3-NOPy moieties. In the calculations given in Fig. 4, we assumed that $k_{1T} = k_{1R} = k_{rel} = 1.9 \cdot 10^7$ s^{-1}. It must be noted that this parameter can be chosen within the interval from ca. $1.5 \cdot 10^6$ to $2.5 \cdot 10^7$ s^{-1}. Varying other parameters accordingly, mainly k_D and k_e, one can maintain nearly the same quality of simulation. It was impossible to fit the experimental kinetics when k_{rel} was beyond this interval.

The rate constants k_D and k_e used to calculate ESP kinetics in Fig. 4 are equal to $2.1 \cdot 10^7$ and $7.5 \cdot 10^6$ s^{-1}, respectively. These parameters agree well with the experimentally determined lifetime of 70 ns [30] of the $|^{(T)}D_{\pm 1/2}\rangle$ spin state. When k_{rel} ranges from $1.5 \cdot 10^6$ to $2.5 \cdot 10^7$ s^{-1}, k_D and k_e are variable within the intervals $(7–25) \cdot 10^6$ and $(7–10) \cdot 10^6$ s^{-1}, respectively.

Neither are the parameters $\xi_{\alpha\beta}$ and ξ_{DQ} unique. For the simulation given in Fig. 4, these parameters are $\xi_{DQ} = 0.68$ and $\xi_{\alpha\beta} = -0.02$. This means that the initial population process of the doublet-quartet manifolds is rather spin selective, i.e., the rate of the direct doublet-doublet population is nearly twice as large as that of spin-forbidden doublet-quartet population. The parameter $\xi_{\alpha\beta}$ is found to be small and negative, i.e., falls in the range $(-0.0006$ to $-0.02)$ depending on the best set of the other parameters. As follows from Eq. (9), the negative sign of this parameter means an initial overpopulation of the $|^{(T)}D_{-1/2}\rangle$ spin state with respect to the $|^{(T)}D_{+1/2}\rangle$ spin state of the doublet subspace of the doublet-quartet manifolds. This agrees with the negative sign of J_{13} and J_{23} obtained in ref. 32.

6 Qualitative Model

Simple analyses of the secular part of the Hamiltonian in the Q-basis as a function of J_e show that there are three points of level crossings. While the energy levels $Q_{-1/2}$ ($Q_{-3/2}$) and $D_{1/2}$ ($D_{-1/2}$) intersect at the common point $J_e = -\omega_0/3$,

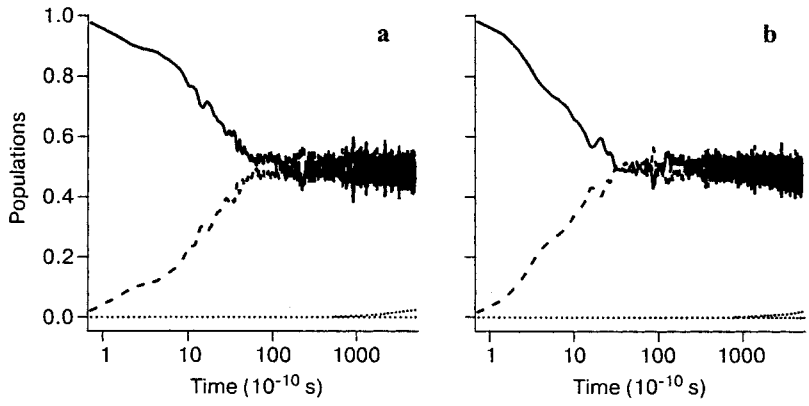

Fig. 5. Relaxation of populations in the vicinity of the level crossings $J_e = -\omega_0/3$ (**a**) and $J_e = -2\omega_0/3$ (**b**). For the former, ${}^{(T)}Q_{-1/2}$ spin state (solid line) is initially populated and comes into equilibrium with the ${}^{(T)}D_{1/2}$ state (dashed line), being much faster than the other spin states (dotted lines). The same is true for the coupling of the ${}^{(T)}Q_{-3/2}$ and ${}^{(T)}D_{-1/2}$ spin states (not shown). For the latter (**b**), the ${}^{(T)}Q_{-3/2}$ state (solid line) is initially populated and comes into equilibrium with the ${}^{(T)}D_{1/2}$ spin state (dashed line), being much faster than the other spin states (dotted lines). Computations were performed with the parameters listed in the legend of Fig. 4, except for the values of k_D (=0) and k_e (=0).

the energy levels $Q_{-3/2}$ and $D_{1/2}$ intersect at $J_e = -2\omega_0/3$. The latter level crossing is called "RTPM crossing" since this crossing plays a dominant role in the creation of CIDEP on encountering of the radicals with molecular triplets [13–15]. Figure 5 demonstrates the increase in the relaxation rates of populations near the crossing points $J_e = -\omega_0/3$ (Fig. 5a) and $J_e = -2\omega_0/3$ (Fig. 5b). In the former case, the ${}^{(T)}Q_{-1/2}$ spin state is initially populated, and in the latter, the ${}^{(T)}Q_{-3/2}$ spin state is initially populated. It is seen from Fig. 5 that crossing states come into an equilibrium much faster than the other spin states. The same is true for the crossing of the ${}^{(T)}Q_{-3/2}$ and ${}^{(T)}D_{-1/2}$ spin states (not shown in Fig. 5). Computations were performed with the parameters listed in the legend of Fig. 4 except the values of k_D (=0) and k_e (=0). For $J_e = -\omega_0/3$, a transient equilibrium occurs between the $Q_{-1/2}$ and $D_{1/2}$ ($Q_{-3/2}$ and $D_{-1/2}$) populations, where the equilibrium populations $\tilde{Q}_{-1/2} = \tilde{D}_{1/2}$ and $\tilde{Q}_{-3/2} = \tilde{D}_{-1/2}$ are equal to $(1 + \xi_{DQ} + 2\xi_{DQ}\xi_{\alpha\beta})/8$ and $(1 + \xi_{DQ} - 2\xi_{DQ}\xi_{\alpha\beta})/8$, respectively. Then, it is easy to find that the intensity of the Q_1 signal at the maximum is proportional to $-(1 - 3\xi_{DQ} + \xi_{DQ}\xi_{\alpha\beta})/4$. Since $\xi_{DQ} > 1/3$ and $|\xi_{\alpha\beta}| \ll 1$, this consideration predicts the positively polarized Q_1 signal. The same consideration predicts that the D_1 signal is proportional to $-\xi_{DQ}\xi_{\alpha\beta}/2$. Since $\xi_{\alpha\beta} < 0$, the D_1 signal has to be positively polarized at the maximum as well. For the RTPM point ($J_e = -2\omega_0/3$) the populations of $Q_{-3/2}$ and $D_{1/2}$ quickly come into an equilibrium with the rate defined by the magnetic interactions of the complex. Hence, one can find that the populations of the cross-levels are equal to $\tilde{Q}_{-3/2} = \tilde{D}_{1/2} = (1 + \xi_{DQ} + 2\xi_{DQ}\xi_{\alpha\beta})/8$. The Q_1 and D_1 signals are proportional to $-3(1 - 3\xi_{DQ} +$

$2\xi_{DQ}\xi_{\alpha\beta})/16$ and $-3(1 - 3\xi_{DQ} + 2\xi_{DQ}\xi_{\alpha\beta})/8$, respective at the maximum. Thus, qualitatively, any level crossing leads to the same time profiles of the Q_1 and D_1 EPR signals. There are two quantitative differences. For the case of the $J_e = -\omega_0/3$ level crossing, the intensity of the Q_1 signal can exceed the intensity of the D_1 signal since $\xi_{DQ}\xi_{\alpha\beta} \ll 1$. For the case of the $J_e = -2\omega_0/3$ RTPM level crossing, the intensity of the Q_1 signal should be about six times greater than that of the D_1 signal. The factor 4 comes from the difference in the transition probabilities of the Q_1 and D_1 transitions [19].

As follows from the calculations, the rates of relaxation transitions $Q_{-1/2} \leftrightarrow D_{1/2}$, $Q_{-3/2} \leftrightarrow D_{-1/2}$, and $Q_{-3/2} \leftrightarrow D_{1/2}$ at the points of level crossing that are induced by ZFS in the rotating ZnTPP-3-NOPy complex are equal to ca. $9 \cdot 10^9$ s^{-1}. The rates of other levels are much slower and lie in the range of $6 \cdot 10^5$ to $9 \cdot 10^5$ for the given magnetic field and the rotational correlation time. As a whole, the system comes into equilibrium with these rates. The rate constants k_e and k_D are found to be also smaller than those of the longitudinal relaxation between the crossing levels. In any case, the rate of depopulation of the $^{(T)}D_{\pm 1/2}$ states, controlled by both the spin-selective (k_D) and spin-nonselective (k_e) intersystem crossing, is faster than the rate of depopulation of $^{(T)}Q_{\pm 1/2}$ and $^{(T)}Q_{\pm 3/2}$, controlled only by the spin-nonselective intersystem crossing. Under these conditions, there exists a time interval when the populations of the $^{(T)}Q_{+3/2}$ and $^{(T)}Q_{+1/2}$ states exceed those

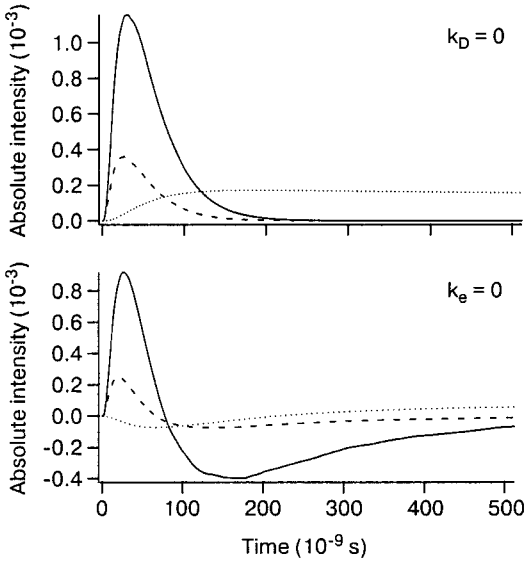

Fig. 6. Computed time profiles of the Q_1 (solid lines), D_1 (dashed lines) and D_0 (dotted lines) EPR signals of the ZnTPP-3-NOPy complex. Parameters used in the calculations are those listed in the legend of Fig. 4, except for $k_D = 0$ (upper, the only spin-nonselective decay) and $k_e = 0$ (lower, the only spin-selective decay). These calculations demonstrate the importance of the suggestion that the doublet and quartet subspaces deactivate with different rates.

of the ${}^{(T)}Q_{-3/2}$ and ${}^{(T)}Q_{-1/2}$ states. This provides the negative sign of TR-ESP (emissive) for the Q_1 and D_1 EPR signals at relatively longer times. It is worthwhile to note that the change in the sign of TR-ESP is of purely kinetic nature and that the nonequivalence in the rates of the intersystem crossings is of critical importance. Figure 6 proves this statement: if $k_D = 0$, the ESP does not change its sign either for the Q_1 or D_1 signal, and if $k_e = 0$, the ratio of the emissive to absorptive signals in their extremes reaches the maximum.

ESP observed for the 3-NOPy moiety (D_0 signal) is due to the transfer of electron polarization from the doublet-quartet manifolds to the $|{}^{(G)}D_{\pm 1/2}\rangle = |G\rangle|\pm 1/2\rangle$ spin states of the complex. Therefore, qualitative interpretation of this polarization is quite clear except for the negative polarization at the short delay time. This negative polarization originates from the fact that the ${}^{(T)}D_{\pm 1/2}$ spin states correlate with the $|{}^{(G)}D_{\pm 1/2}\rangle = |S\rangle|\pm 1/2\rangle$ spin states. At the same time, the ${}^{(T)}D_{\pm 1/2}$ spin states contain excesses (Eq. (2)) of the $|\mp 1/2\rangle$ spins states of s_3 spin, respectively. This is why the quickly created excess of the ${}^{(T)}D_{-1/2}$ population is transferred to the $|+1/2\rangle$ spin state of 3-NOPy [22, 24]. At later time, the contribution from the quartet subspace dominates because of the faster depopulation of the doublet subspace. Positive ESP of the D_0 signal arises from this domination. The final negative polarization is due to the change in Q_1 polarization.

7 Conclusion

A theoretical model for the formation of ESP in the ZnTPP-3-NOPy complex is suggested. Conceptually, the present model differs from the models that were previously suggested for RTPM in liquid solution by constancy of the Heisenberg spin exchange interaction in the system. Numerical simulations showed that there are three necessary conditions for an observation of TR-ESP in the system. First, in accordance with the exchange mechanism [1–4] the initial population of the doublet subspace exceeds the initial population of the quartet subspace. Second, rates of longitudinal relaxation due to ZFS in a rotating complex are selective to the spin states because of different energy separations. This results in a pseudo-equilibrium characterized by nonzero longitudinal magnetizations belonging to different subspaces. Third, the rates of the depopulation (relaxation) of the different subspaces are different as well. The doublet subspace deactivates faster than the quartet subspace does.

However, it follows from computations that these conditions are necessary but not sufficient to get successful numerical modeling. It was found that the additional internal paramagnetic relaxation must be taken into consideration. Most likely this internal relaxation is due to relative motion of the ZnTPP and 3-NOPy moieties. It was also found that there must be small but nonzero excess populations of the ${}^{(T)}D_{-1/2}$ spin state over its ${}^{(T)}D_{+1/2}$ partner in the initial stage.

In order to attain more unique simulations we have to determine some of the relaxation parameters by other independent experiments.

Appendix

In the τ-basis ($|\tau_\mu(1,2)\chi_m(3)\rangle; \hat{S}_\mu |\tau_\mu(1,2)\rangle = 0$), the generalized relaxation matrix $\hat{\hat{R}}_{1/2}$ for the spin 1/2 (3-NOPy) is given by

$$\hat{\hat{R}}_{1/2} = \begin{pmatrix} -k_{1R} & 0 & 0 & k_{1R} \\ 0 & -k_{2R} & 0 & 0 \\ 0 & 0 & k_{2R} & 0 \\ k_{1R} & 0 & 0 & -k_{1R} \end{pmatrix}. \tag{A1}$$

For the spin 1 (molecular triplet of ZnTPP) we use the generalized matrix

$$\hat{\hat{R}}_1 = \begin{pmatrix} -2k_{1T} & 0 & 0 & 0 & k_{1T} & 0 & 0 & 0 & k_{1T} \\ 0 & k_{2T} & 0 & 0 & 0 & 0 & 0 & 0 & 0 \\ 0 & 0 & k_{2T} & 0 & 0 & 0 & 0 & 0 & 0 \\ 0 & 0 & 0 & k_{2T} & 0 & 0 & 0 & 0 & 0 \\ k_{1T} & 0 & 0 & 0 & -2k_{1T} & 0 & 0 & 0 & k_{1T} \\ 0 & 0 & 0 & 0 & 0 & k_{2T} & 0 & 0 & 0 \\ 0 & 0 & 0 & 0 & 0 & 0 & k_{2T} & 0 & 0 \\ 0 & 0 & 0 & 0 & 0 & 0 & 0 & k_{2T} & 0 \\ k_{1T} & 0 & 0 & 0 & k_{1T} & 0 & 0 & 0 & -2k_{1T} \end{pmatrix}. \tag{A2}$$

From Eqs. (A1) and (A2) the generalized 36-dimensional relaxation matrix $\hat{\hat{R}}$ is obtained for the doublet-quartet manifolds in the τ-basis. This relaxation matrix describes the relaxation process only qualitatively. It is worthwhile to note that such a relaxation matrix is unique for a given basis.

Acknowledgments

This research was supported by the Russian Foundation for Basic Research (05-03-32197-a, 04-03-32604-a, and 06-03-91362-a), the German Research Foundation (SPP 1051, SFB 498, MO 132/19-2), and the Japan Society for the Promotion of Science (Japan-Russia Joint Research Project 6037711-361). This paper is dedicated to Kev Salikhov (Kazan) on the occasion of his 70th birthday.

References

1. Hoijtink G.J.: Mol. Phys. **3**, 67 (1960)
2. Murrell J.N.: Mol. Phys. **3**, 317 (1960)
3. Robinson G.W.: J. Mol. Spectrosc. **6**, 58 (1961)

4. Chiu Y.-N.: J. Chem. Phys. **56**, 4882 (1972)
5. Step E.N., Buchachenko A.L., Turro N.J.: J. Am. Chem. Soc. **116**, 5462 (1994)
6. Magin I.M., Purtov P.A., Kruppa A.I., Leshina T.V.: Appl. Magn. Reson. **26**, 155 (2004)
7. Magin I.M., Purtov P.A., Kruppa A.I., Leshina T.V.: J. Phys. Chem. A **109**, 7396 (2005)
8. Blättler C., Jent F., Paul H.: Chem. Phys. Lett. **166**, 375 (1990)
9. Jenks W.S., Turro N.J.: Res. Chem. Intermed. **13**, 237 (1990)
10. Kawai A., Okutsu T., Obi K.: J. Phys. Chem. **95**, 9130 (1991)
11. Saiful I.M., Fujisawa J., Kobayashi N., Ohba Y., Yamauchi S.: Bull. Chem. Soc. Jpn. **72**, 661 (1999)
12. Blank A., Levanon H.: J. Phys. Chem. A **105**, 4799 (2001)
13. Shushin A.I.: Chem. Phys. Lett. **313**, 246 (1999); J. Chem. Phys. **99**, 8723 (1993)
14. Imamura T., Onitsuka O., Obi K.: J. Phys. Chem. **90**, 6741 (1986)
15. Fujisawa J., Ohba Y., Yamauchi S.: J. Phys. Chem. A **101**, 434 (1997)
16. Closs G.L., Gautam P., Zhang D., Crusic P., Hill S.A., Wasserman E.: J. Phys. Chem. **96**, 5528 (1992)
17. Regev A., Gamkiel D., Meiklyer V., Michaeli S., Levanon H.: J. Phys. Chem. **97**, 3671 (1993)
18. Corvaja C., Maggini M., Prato M., Scorrano G., Venzin M.: J. Am. Chem. Soc. **117**, 8858 (1995)
19. Fujisawa J., Ishii K., Ohba Y., Yamauchi S., Fuhs M., Möbius K.: J. Phys. Chem. A **103**, 213 (1997)
20. Ishii K., Fujisawa J., Adachi A., Yamauchi S., Kobayashi N.: J. Am. Chem. Soc. **120**, 3152 (1998)
21. Tarasov V.F., Shkrob I.A., Trifunac A.D.: J. Phys. Chem. A **106**, 4838 (2002)
22. Corvaja C., Maggini M., Ruzzi M., Scorrano G., Toffoletti A.: Appl. Magn. Reson. **12**, 477 (1997)
23. Iwasaki Y., Katano K., Ohba Y., Karawasa S., Koga N., Yamauchi S.: Appl. Magn. Reson. **23**, 377 (2003)
24. Salikhov K.M., van der Est A.J., Stehlik D.: Appl. Magn. Reson. **16**, 101 (1999)
25. Fujisawa J., Iwasaki Y., Ohba Y., Yamauchi S., Koga N., Karasawa S., Fuhs M., Möbius K., Weber S.: Appl. Magn. Reson. **21**, 483 (2001)
26. Yamauchi S.: Bull. Chem. Soc. Jpn. **77**, 1255 (2004)
27. Mahler G., Weberruß V.A.: Quantum Networks: Dynamics of Open Nanostructures. Berlin: Springer 1995.
28. Tarasov V.V.: Ph.D. thesis, University of Zürich, Zürich, Switzerland, 1999.
29. Kollimar C., Sixl H.: Mol. Phys. **45** 1199 (1982)
30. Ishii K., Ohba B., Iwaizumi M., Yamauchi S.: J. Phys. Chem. **100**, 3839 (1996)
31. Yamauchi S., Maretti L., Saiful I.S.M., Iwasaki Y., Ohba Y. in: Book of Abstracts, 9th International Symposium on Spin and Magnetic Field Effects in Chemistry and Related Phenomena, 11–17 September 2005, p. 137. Oxford: University of Oxford.

Authors' address: Valery F. Tarasov, Institute of Chemical Physics, Russian Academy of Sciences, ulitsa Kocygina 4, Moscow 199991, Russian Federation